JOURNAL OF VIROLOGY, Jan. 1994, p. 328–337
0022-538X/94/$04.00+0

Vol. 68, No. 1

Optimization of Targeted RNA Recombination and Mapping of a Novel Nucleocapsid Gene Mutation in the Coronavirus Mouse Hepatitis Virus

PAUL S. MASTERS,[1,2]* CHERI A. KOETZNER,[1] CHERYL A. KERR,[1] AND YONG HEO[2]

Wadsworth Center for Laboratories and Research, New York State Department of Health, Albany, New York 12201,[1] and Department of Biomedical Sciences, School of Public Health, State University of New York at Albany, Albany, New York 12237[2]

Received 20 July 1993/Accepted 8 October 1993

We have recently described a method of introducing site-specific mutations into the genome of the coronavirus mouse hepatitis virus (MHV) by RNA recombination between cotransfected genomic RNA and a synthetic subgenomic mRNA (C. A. Koetzner, M. M. Parker, C. S. Ricard, L. S. Sturman, and P. S. Masters, J. Virol. 66:1841–1848, 1992). By using a thermolabile N protein mutant of MHV (Alb4) as the recipient virus and synthetic RNA7 (the mRNA for the nucleocapsid protein N) as the donor, we selected engineered recombinant viruses as heat-stable progeny resulting from cotransfection. We have now been able to greatly increase the efficiency of targeted recombination in this process by using a synthetic defective interfering (DI) RNA in place of RNA7. The frequency of recombination is sufficiently high that, with Alb4 as the recipient, recombinants can be directly identified without using thermal selection. The synthetic DI RNA has been used to demonstrate that the lesion in another temperature-sensitive and thermolabile MHV mutant, Alb1, maps to the N gene. Sequencing of the Alb1 N gene revealed two closely linked point mutations that fall in a region of the N molecule previously noted as being the most highly conserved region among all of the coronavirus N proteins. Analysis of revertants of the Alb1 mutant revealed that one of the two mutations is critical for the temperature-sensitive phenotype; the second mutation is phenotypically silent.

The unique genomic composition of RNA viruses puts them in a singular category with respect to the molecular genetic methods that may be applied to their study. RNA is much more chemically labile than DNA, and, with few exceptions, the techniques available for the engineering of recombinant DNA as yet have no counterparts for RNA. The obstacles that this presents to genetic manipulation are probably least for the positive-strand RNA viruses, which have the advantage that their genomes, in isolation, are infectious when introduced into susceptible host cells.

A major advance in RNA virology was made by the assembly of a full-length, infectious cDNA clone of poliovirus (28). This enabled the site-specific mutagenesis of the poliovirus genome by means of a DNA proxy, and it provided a strategy that was, in principle, applicable to all other positive-strand RNA viruses. Subsequently, infectious RNAs for a number of viruses of this class have been successfully produced. Two major constraints on this approach are the size of the viral genome and how precisely its 5′ and 3′ termini must be tailored. Many problems associated with the latter were alleviated by the advent of the use of bacteriophage RNA polymerases for in vitro RNA synthesis (25). Genome size, however, remains a formidable obstacle: to date, the largest cloned and expressed RNA genome is that of Sindbis virus, which is 11.7 kb (30).

Coronaviruses are positive-strand RNA viruses with genomes of 26 to 31 kb, the largest coding capacities known for any RNA viruses. Their replication involves leader RNA-primed synthesis of a 3′-nested set of subgenomic mRNAs (18, 39, 41). Thus, coronavirus subgenomic RNAs contain the same 5′ and 3′ termini as the full-length genome. As well, each of these species has a negative-strand RNA counterpart, and consequently each is potentially a replicative entity (34, 37). A further remarkable feature of coronavirus RNA synthesis is the high rate of homologous RNA recombination that occurs during replication (4; reviewed in reference 17), probably by means of a template-switching mechanism.

The enormous size of coronavirus genomes makes the production and manipulation of full-length infectious RNAs unlikely in the near term. However, RNA recombination may be exploited to circumvent this limitation. We (16) and another group (42) have demonstrated that site-specific mutations can be introduced into the 3′ end of the genome of the coronavirus mouse hepatitis virus (MHV) by transfection of RNA into cells cotransfected or infected with an MHV mutant containing a rescuable mutation in the nucleocapsid (N) gene, the gene closest to the 3′ terminus of the virus. In our case, the donor RNA used was a synthetic copy of subgenomic RNA7, the mRNA for the N protein (16). In a very similar selection, Van der Most et al. (42) used a derivative of a cloned MHV defective interfering (DI) RNA containing a fragment of the N gene as the donor RNA and obtained recombinants at a considerably higher frequency. MHV DI RNAs are extensively deleted genome-derived RNAs that are replication competent but can replicate only at the expense of a coinfecting helper virus. Those that have been characterized contain intact 5′- and 3′-terminal portions of the MHV genome as well as one or more discontinuous internal segments (7, 12, 15, 18, 42).

In this report, we describe the construction of a synthetic DI RNA as an optimized vector for targeted RNA recombination with the MHV genome and demonstrate its use in mapping a novel N gene mutation in MHV.

* Corresponding author. Mailing address: Wadsworth Center, New York State Department of Health, Albany, NY 12201-0509. Phone: (518) 474-1283. Fax: (518) 473-1326.

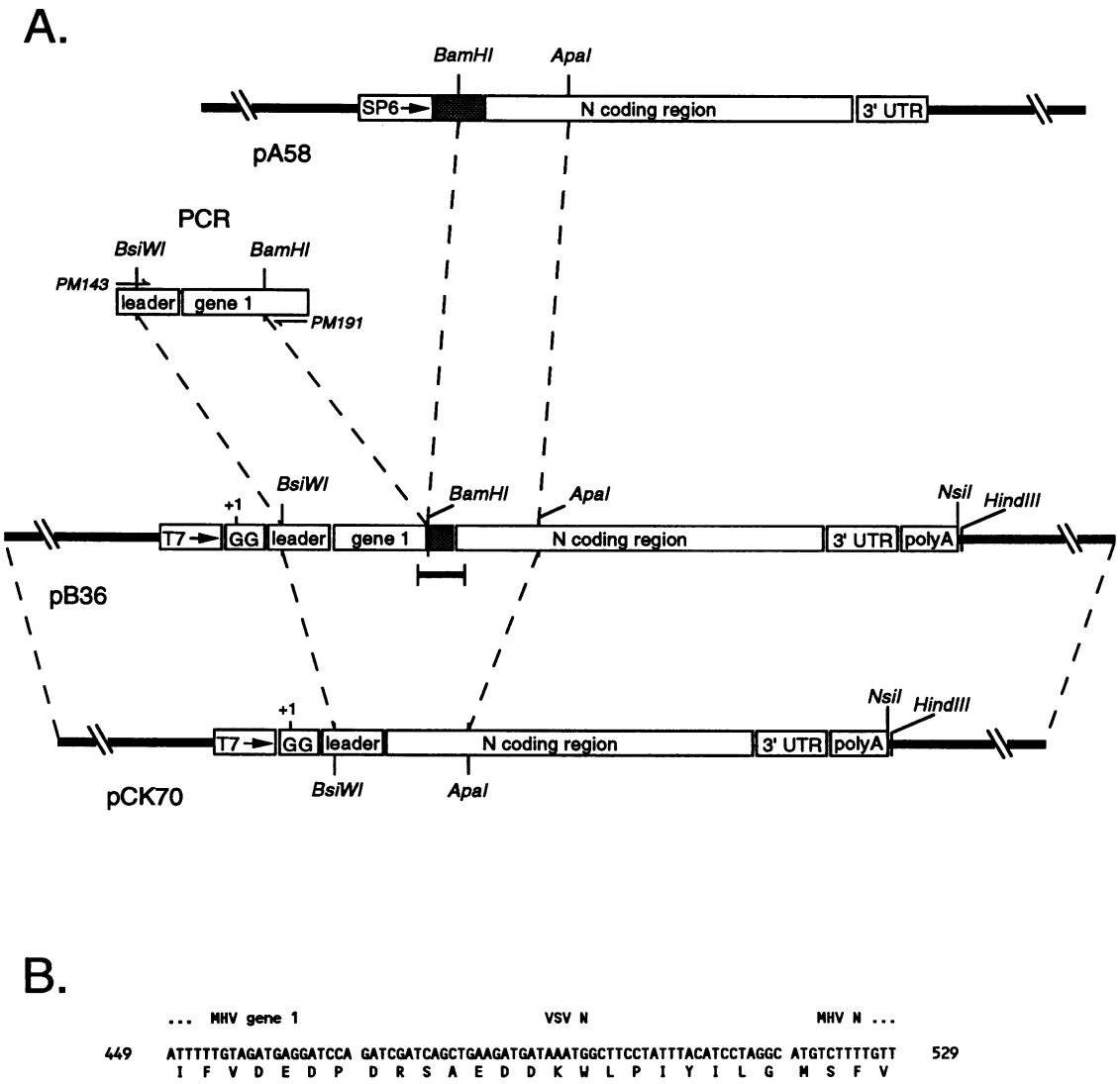

FIG. 1. Construction of a transcription vector used for the synthesis of synthetic MHV DI RNA. (A) Schematic of the strategy for the construction of the vector pB36, as detailed in Materials and Methods. (B) Sequence of the junctions of pB36 at which gene 1 of MHV is fused, in frame, to a short region of heterologous material from the VSV N gene followed, in frame, by the complete coding region of the MHV N gene. Nucleotide numbering begins with the first base of the encoded T7 polymerase-transcribed DI RNA.

MATERIALS AND METHODS

Virus and cells. MHV-A59 wild-type, mutant, and recombinant virus stocks were grown in mouse 17 clone 1 (17Cl1) cells; plaque titer determinations and plaque purifications were performed in mouse L2 cells. Spinner cultures of L2 cells were maintained in Joklik's minimal essential medium (MEM) containing 10% fetal bovine serum at densities between 1×10^5 and 2×10^6 cells per ml. Thermal inactivation of wild-type and mutant viruses was carried out at 40°C and pH 6.5 as described previously (16).

Construction of synthetic DI vector. A vector, pB36, expressing a synthetic MHV DI RNA species under the control of a T7 RNA polymerase promoter, was constructed from pCK70, which had been used previously to express MHV subgenomic RNA7 (16). The portion of pCK70 between the *Bsi*WI and *Apa*I sites was replaced in a three-way ligation with (i) a fragment corresponding to the 5′ end of the MHV genome plus (ii) a piece of a heterologous gene fused in frame to the 5′ end of the MHV N coding region (Fig. 1A). The MHV genomic 5′-end fragment was obtained by polymerase chain reaction (PCR) amplification of cDNA prepared from wild-type MHV-A59 genomic RNA by using primer PM 191, complementary to nucleotides (nt) 505 to 522 of the MHV genome, and primer PM143, corresponding to nt 1 to 28 of the MHV genome (26). The PCR product was restricted with *Bsi*WI and *Bam*HI. The MHV N gene 5′-end fusion fragment was the *Bam*HI-*Apa*I fragment of pA58, which contains two small discontinuous portions of the vesicular stomatitis virus (VSV) N gene fused to the 5′ end of the MHV N gene coding region (23). The resulting construct, pB36, when truncated with *Nsi*I, acted as the template for synthesis of a runoff RNA consisting of two 5′ G residues preceding nt 1 to 467 of the MHV genome, followed by nt 373 to 420 of the coding region of the VSV N gene (3), followed by the entire MHV N gene,

3′ untranslated region (UTR), and a poly(A) tract of 100 to 110 residues (16). Recombinant DNA manipulations were carried out by standard techniques (31); PCRs were as described previously (16). The PCR-generated segment and all newly created junctions of pB36 were verified by DNA sequencing. Plasmid pB36 contained three base differences with respect to the previously reported sequence for the 5′ end of MHV-A59 (26): nt 151 was C instead of T, nt 179 was C instead of G, and nt 416 was A instead of G. Only the last of these fell in the coding region for gene 1, where it resulted in a silent codon change; the base difference at nt 179 was identical to that in MHV-JHM (37).

Genome RNA purification and synthesis of subgenomic and DI RNA. The preparation of viral genomic RNA from virus that was purified on potassium tartrate-glycerol gradients was performed exactly as described previously (16). Yields of genomic RNA were quantitated by measurement of A_{260}. Subgenomic RNA7 and DI RNA were synthesized as capped runoff transcripts from *Nsi*I-truncated pCK70 and pB36, respectively, essentially as described by Melton et al. (25). Cap analog m^7GpppG and T7 RNA polymerase were obtained from New England BioLabs; RNasin was obtained from Promega. RNA products were purified with RNaid (Bio 101, Inc.). The yield of RNA synthesis reactions was monitored by incorporation of [5,6-^{3}H]UTP (Amersham) in parallel reactions, as determined by binding of product RNA to DEAE filter paper (Whatman DE 81).

Transfection and recombinant selection. RNA transfections were performed by electroporation under conditions similar to those described by Liljeström et al. (21) for Semliki Forest virus RNA. L2 cells growing in spinner culture were harvested at a density of 4×10^5 to 8×10^5 cells per ml, washed once with calcium- and magnesium-free phosphate-buffered saline at ambient temperature, and resuspended in the same buffer to a density of 5×10^6 to 8×10^6 cells per ml. Cells (0.4 ml) were mixed with RNA (10 to 40 μl), transferred to a 0.2-cm cuvette, and electroporated at ambient temperature with two consecutive pulses from a Bio-Rad Gene Pulser apparatus set at 0.8 kV and 25 μF, with a Bio-Rad Pulse Controller set at maximum resistance. Transfected cells were then diluted into 8 ml of Dulbecco's MEM and plated onto two 20-cm^2 confluent monolayers of 17Cl1 cells. For experiments directly comparing subgenomic RNA7 and DI RNA, synthetic RNA was cotransfected at the indicated molar ratio with 2 μg of Alb4 genomic RNA. For mapping experiments, L2 cells grown in spinner culture were harvested, resuspended in Joklik's MEM to a density of 1×10^7 cells per ml, and infected in suspension at a multiplicity of ca. 0.5 PFU per cell with the indicated MHV mutant. Following 2 h of incubation at 33°C, cells were washed and electroporated with 0.05 or 0.5 μg of synthetic RNA as above.

Cotransfected or infected/transfected L2 cells were incubated at 33°C until extensive syncytia and cytopathic effect appeared on the secondary 17Cl1 monolayers (24 to 30 h posttransfection or postinfection). Titers of released progeny virus were determined at the indicated temperature with or without prior thermal inactivation.

Labeling of viral RNA. Virus-specific RNA in infected/transfected cells was metabolically labeled with $^{32}P_i$ by a method similar to previously published procedures (22, 33). In brief, spinner culture L2 cells were infected in suspension with wild-type MHV at a multiplicity of 1 PFU per cell. Following 2 h of incubation at 37°C, cells were washed; electroporated with 0, 0.5, 1.0, or 1.5 μg of unlabeled synthetic DI RNA as described above; and plated onto a 20-cm^2 confluent monolayer of 17Cl1 cells at 37°C. A mock-infected, mock-transfected control sample was treated identically. Cells were incubated from 11 to 13 h postinfection in Eagle's MEM containing 1/10 of the normal phosphate concentration and 5% dialyzed fetal bovine serum. They were then labeled from 13 to 15 h postinfection by incubation with 1 ml of phosphate-free Eagle's MEM containing 5% dialyzed fetal bovine serum, 333 μCi of $^{32}P_i$ (Amersham), and 20 μg of actinomycin D (Merck) per ml. Total cytoplasmic RNA was purified, and equal fractions of each sample were analyzed by electrophoresis on a 1% agarose gel containing formaldehyde (31) and visualized by autoradiography.

Cloning and sequencing of the N genes of Alb1 and its revertants. cDNA clones of the N gene and part of the M gene of the Alb1 mutant were generated from purified genomic RNA. First- and second-strand cDNAs were synthesized by a modification of the procedure of Gubler and Hoffman (10), and the *Kpn*I-*Sac*I fragment running from the middle of the M gene to the distal portion of the 3′ UTR was cloned into the vector pGEM-7Zf(+) (Promega), which had been restricted with *Kpn*I and *Sac*I. The sequence of the entire cloned region of Alb1 was determined at least once in both directions from a single plasmid, pCK31, and the two nucleotide differences from the wild-type sequence were then confirmed on four independent cDNA clones. DNA sequencing was carried out by the method of Sanger et al. (32) with modified T7 DNA polymerase (Sequenase; U.S. Biochemical) and primers described previously (27).

Independent revertants of Alb1 were isolated as large-plaque survivors of a 24-h thermal inactivation of stocks of Alb1 that had been passaged twice at the nonpermissive temperature, 39°C. Each revertant (designated Alb1Rev) was obtained from a virus stock that had originated from an independent plaque of Alb1. Alb1RevA-Alb1RevB and Alb1RevC-Alb1RevN arose from two separate searches.

The entire N gene and partial M gene sequences of Alb1RevA and Alb1RevB were determined from cDNA clones as described above for Alb1, except that the cloned *Kpn*I-*Sac*I fragment was obtained by reverse transcription followed by PCR. The relevant portion of the Alb1RevA N sequence was confirmed on two additional clones; the relevant portion of the Alb1RevB N sequence was confirmed by sequencing RNA from infected cells. For Alb1RevC-Alb1RevN and for serially passaged Alb1RevA, the region of the N gene encompassing the Alb1 mutations was sequenced on RNA from infected cells by a modification of the procedure of Fichot and Girard (9) with a primer complementary to nt 469 to 486 of the N gene sequence (27).

RESULTS

Optimization of targeted recombination. In previous work we demonstrated that targeted recombination could be carried out between MHV genomic RNA and cotransfected synthetic RNA7, the smallest of the subgenomic mRNAs of MHV (16). This system made use of a thermolabile mutant with a deletion mutation in the MHV N gene, Alb4, which allowed a powerful counterselection for engineered recombinant viruses. Although this technique has been used subsequently to construct a number of novel N protein mutants (24), it was consistently noted to have a low efficiency. We previously estimated that recombinants were recovered at a frequency on the order of 10^{-5}. Routinely, we observed that only a few of a large number of replicate cotransfections yielded recombinants. One consequence of this was that it could not be determined with confidence whether failure to incorporate a particular mutation into the MHV genome indicated failure to cross the

threshold of detection or whether the mutation being sought was lethal.

In an attempt to optimize the conditions for targeted recombination, we focused on two aspects of the process: the efficiency of RNA transfection and the donor RNA species. The RNA transfection efficiency was markedly improved through transfection of cells grown in spinner culture. We had previously observed that higher transfection efficiencies were obtained with trypsinized cells transfected in suspension, compared with cells in monolayer. However, trypsinization of cell monolayers had poor day-to-day reproducibility. To obviate this source of variability, we used mouse L2 cells, which are a suitable host for MHV and which have the advantage that they can be grown in either spinner or monolayer culture, depending on the medium. The method of RNA transfection that, in our hands, gave the best and most reproducible results was electroporation, carried out under conditions that have been recently described for high-efficiency transfection of Semliki Forest virus RNA (21). Following electroporation of MHV RNA into L2 cells grown in spinner culture, these cells were plated onto monolayers of 17Cl1 cells. The appearance of extensive syncytia on the latter, following 24 to 30 h incubation at 33°C, indicated that successful transfection followed by secondary infection had occurred.

This transfection technique consistently yielded infections with kinetics and extents similar to those brought about by infection with whole virus, suggesting that the efficiency of introduction of genomic and subgenomic MHV RNA into cells was not rate limiting in our ability to obtain recombinants. However, since the observed frequency of recombination was not measurably improved, we sought to optimize the donor RNA. For this purpose, we constructed a vector for synthesis of a transcript meant to function as an MHV DI RNA. This was motivated by two considerations. First, Van der Most et al. (42) have demonstrated a very high frequency of repair of the Alb4 deletion mutation by using a vector derived from a naturally arising MHV DI RNA. Second, the work of other investigators (6, 12) has raised the possibility that MHV subgenomic RNAs do not function as independent replicons. By their models, subgenomic RNA7 would act as template for synthesis of negative-strand RNA molecules, but these molecules would not amplify further. Hence, opportunities for recombination with the MHV genome would be limited for RNA7 compared with those open to a fully replicating DI RNA molecule.

The synthetic MHV DI that we constructed was patterned after a naturally arising bovine coronavirus (BCV) DI RNA discovered by Chang and Brian (6), in which the first 498 nt of the BCV genome is fused to the 3′ end of the BCV genome, beginning exactly with the start codon of the N gene. This replicating species encodes a fusion protein consisting of the first 96 amino acids of the BCV gene 1 product followed by the entire BCV N protein. We constructed a vector for an approximate MHV analog of this by incorporating the first 467 nt of the MHV genome into pCK70, the transcription vector for synthetic RNA7 (Fig. 1A). This was linked, via a short fragment of heterologous sequence (derived from the VSV N gene), to the 3′ end of the MHV genome, beginning exactly with the start codon of the N gene. The resulting construct, pB36, contained a large open reading frame encoding the first 86 residues of the MHV gene 1 protein, which was fused to residues 125 to 140 of the VSV N protein, which was fused, in turn, to the entire MHV N protein (Fig. 1B). The construct was designed in this manner in light of accumulating results showing that, for unknown reasons, the maintenance of a continuous large open reading frame is critical for the replicative ability of MHV DIs (7, 15).

The relative abilities of synthetic RNA7 and DI RNA to act as donors for recombination with the N gene deletion mutant Alb4 were then tested. Alb4 forms tiny plaques at the nonpermissive temperature (39°C) (16). It is also thermolabile in that its virions undergo a drop in titer that is orders of magnitude greater than that of wild-type virions after 24 h of incubation at the nonpermissive temperature (16). To compare the two donor RNA species, synthetic RNA7 or DI RNA was mixed, at various molar ratios, with purified Alb4 genomic RNA and cotransfected into cells. Recombinant viruses were scored as large (wild-type-sized) plaques among progeny virus whose titer had been determined, with or without prior thermal inactivation. One such comparison is shown in Table 1. In this particular experiment none of the three samples in which RNA7 was used as donor RNA yielded a detectable level of recombinants. There was also no detectable frequency of revertants in control samples that did not receive synthetic RNA. By contrast, cotransfection with DI RNA produced recombinants at a frequency as much as 120-fold higher than the upper limit of recombination that could be set for samples cotransfected with RNA7. The highest frequency of recombinants was obtained at an input RNA molar ratio of 0.1 (ratio of DI to genomic RNA), and this trend has held in subsequent experiments to construct other recombinants. However, it must be noted that the given RNA molar ratios provide a working basis for comparison, but it is not known what fraction of purified viral genomic RNA is actually infectious. Thus, the molar ratios with respect to actually functional RNA species may be much higher.

As shown in Table 1, with cotransfected DI RNA, recombinants occurred in sufficiently large numbers to allow their identification without selection by thermal inactivation. In the experiment shown, up to 10% of total unselected plaques obtained from cotransfected DI RNA were recombinants. Heat selection, however, greatly reduced the background of small plaques, and large-plaque recombinants could be found to constitute as much as 80% of plaques surviving thermal inactivation (Table 1).

Table 1 also shows that, for the largest amount of cotransfected DI RNA, there was a significant inhibition of titer of progeny virus compared with controls that received no synthetic RNA. The kinetics of infection for this sample were also markedly slower than for the controls. This effect has been noted consistently in numerous experiments (see also Table 2), and it suggests that the pB36-derived RNA is truly functioning as a DI RNA. By contrast, we have consistently noted that the kinetics and yield of cotransfections with RNA7 are increased with respect to those of controls. It is not known whether this effect is limited to Alb4, but it may suggest that cotransfected RNA7 is functioning primarily as an mRNA for N protein synthesis, which then enhances MHV infection by an unknown mechanism.

Mapping of MHV mutations. Within a previously isolated set of 24 temperature-sensitive mutants of MHV-A59 (40), three mutants, Alb1, Alb4, and Alb25, were noteworthy for the extreme thermolability of their virions. Alb1 and Alb25 were found to have a phenotype very similar to that previously reported for the N mutant Alb4 (16). At the nonpermissive temperature, 39°C, Alb1 and Alb25 formed very tiny plaques (0.5 to 1.0 mm in diameter after 48 h, compared with 1.0 to 1.5 mm for Alb4 and 3.5 to 4.0 mm for the wild type). Thermal inactivation of Alb1 and Alb25 at 40°C, measured over the course of 24 h, is shown in Fig. 2. Because these inactivation profiles closely resembled each other, as well as that of Alb4,

TABLE 1. Comparison of synthetic RNA7 and DI RNA as donors in targeted recombination with Alb4 as the recipient[a]

Donor RNA	Molar ratio of donor to genomic RNA	Titer (PFU/ml) at 39°C		Frequency of large plaques[b]
		Small plaques	Large plaques	
Following thermal inactivation[c]				
None	0:1	2.8×10^4	ND[d] ($<10^2$)	ND ($<10^{-4}$)
None	0:1	2.6×10^4	ND ($<10^2$)	ND ($<10^{-4}$)
RNA7	0.1:1	5.7×10^4	ND ($<10^2$)	ND ($<10^{-4}$)
RNA7	1:1	7.8×10^4	ND ($<10^2$)	ND ($<10^{-4}$)
RNA7	10:1	1.7×10^5	ND ($<10^2$)	ND ($<10^{-4}$)
DI RNA	0.1:1	2.5×10^4	2.0×10^4	1.2×10^{-2}
DI RNA	1:1	2.9×10^4	2.5×10^3	1.3×10^{-3}
DI RNA	10:1	5.2×10^3	1.2×10^3	5.2×10^{-3}
Without thermal inactivation				
None	0:1	2.3×10^6	ND ($<10^3$)	ND ($<10^{-3}$)
None	0:1	9.5×10^5	ND ($<10^3$)	ND ($<10^{-3}$)
RNA7	0.1:1	1.6×10^6	ND ($<10^3$)	ND ($<10^{-3}$)
RNA7	1:1	2.2×10^6	ND ($<10^3$)	ND ($<10^{-3}$)
RNA7	10:1	2.9×10^6	ND ($<10^3$)	ND ($<10^{-3}$)
DI RNA	0.1:1	1.5×10^6	1.9×10^5	1.1×10^{-1}
DI RNA	1:1	1.9×10^6	7.3×10^3	3.8×10^{-3}
DI RNA	10:1	2.3×10^5	3.3×10^3	1.4×10^{-2}

[a] Alb4 genomic RNA and synthetic RNA7 or DI RNA (or H_2O as control) were cotransfected into L2 cells by electroporation, and transfected L2 cells were then plated onto a monolayer of 17 clone 1 cells, as described in Materials and Methods. Progeny virus titers were determined on L2 cell monolayers with or without prior thermal inactivation.

[b] Defined as the titer of large plaques at 39°C divided by the total titer (large plus small plaques) at 39°C without prior thermal inactivation.

[c] At 39°C for 24 h.

[d] ND, not detected.

this raised the possibility that the extreme thermolability phenotype was a hallmark of MHV N protein mutants. To test this notion, we carried out targeted recombination with synthetic DI RNA in an attempt to map the mutations in these viruses. At the time these experiments were begun, Alb1 was known to contain two point mutations in its N gene, but it had not been ascertained whether these were related to its phenotype.

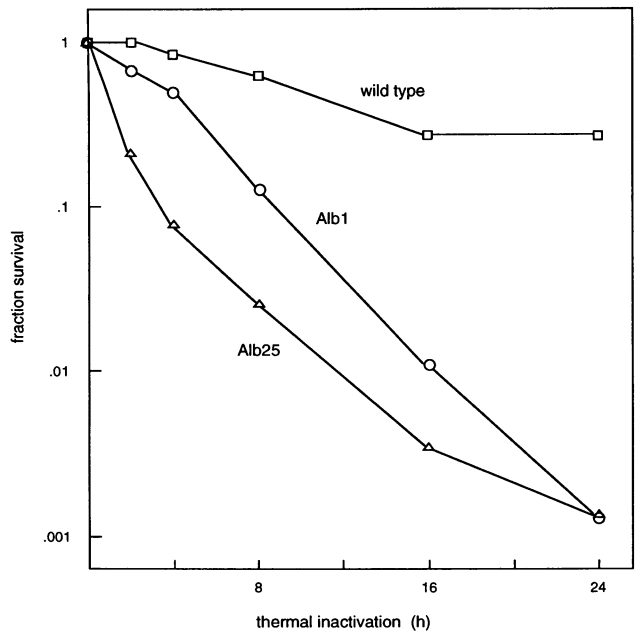

FIG. 2. Thermolability of virions of two mutants, Alb1 and Alb25. Viruses were thermally inactivated at 40°C (pH 6.5) for the indicated times, as described previously (16). Titers of surviving viruses were determined at 33°C. The control inactivation profile for wild-type virus has been presented previously (16).

Mapping experiments were performed by a modified method involving infection followed by transfection to establish conditions that potentially could be applied to other mutants in the future without the necessity for purifying viral genomic RNA. L2 cells were infected in suspension with a low-passage stock of Alb1 or Alb25, and at 2 h postinfection the cells were electroporated with two different amounts of DI RNA (or H_2O as a control). Titers of progeny viruses resulting from this infection were determined at the nonpermissive temperature to find whether recombinants had been generated. To assay the reliability of this protocol, we used Alb4 as a positive control. For a negative control, we used Alb18, a known temperature-sensitive conditional-lethal S protein mutant (29). Table 2 shows the results of one of a number of mapping experiments that were done. As expected, Alb4 had an undetectable background of reversion and gave rise to recombinants at a rate that increased with the amount of input transfected pB36-derived DI RNA. Alb18, which has a single point mutation in the first half of the S gene, also did not have a detectable level of reversion under the conditions of the mapping experiment. Transfection of DI RNA into Alb18-infected cells did not give rise to large plaques at the nonpermissive temperature, ruling out the possibility that DI RNA transfection somehow increased the rate of reversion of mutants. The mutant Alb1 had an undetectable level of reversion and gave rise to recombinants with transfected DI RNA, and thus, like Alb4, its lesion clearly maps to the N gene. By contrast, the reversion rate of Alb25 defined the limit of the mapping procedure. In multiple experiments with this mutant, we never observed a rate of recombination significantly higher than the rate of reversion. Similarly indeterminate results were obtained when infections were repeated with three independent passage 1 stocks, each of which had been begun from a

TABLE 2. Mapping of MHV-A59 mutations with pB36-derived DI RNA[a]

Recipient virus	Amt of transfected DI RNA (μg)	Titer (PFU/ml)	
		Total plaques (33°C)	Large plaques (39°C)
Alb1	0	2.0×10^7	ND[b] ($<10^3$)
Alb1	0.05	2.2×10^7	2.0×10^3
Alb1	0.5	1.5×10^7	5.3×10^3
Alb4	0	1.4×10^7	ND ($<10^3$)
Alb4	0.05	1.4×10^7	1.0×10^3
Alb4	0.5	1.2×10^7	3.3×10^3
Alb18	0	2.2×10^7	ND ($<10^3$)
Alb18	0.05	2.5×10^7	ND ($<10^3$)
Alb18	0.5	7.5×10^6	ND ($<10^3$)
Alb25	0	8.3×10^6	8.7×10^4
Alb25	0.05	7.2×10^6	1.3×10^5
Alb25	0.5	4.7×10^6	2.0×10^4

[a] L2 cells were infected with mutant virus and then transfected with the indicated amount of DI RNA or with H_2O as a control. Transfected L2 cells were then plated onto a monolayer of 17 clone 1 cells, as described in Materials and Methods, and progeny virus titers were determined on L2 cell monolayers at both the permissive temperature (33°C) and the nonpermissive temperature (39°C) without prior thermal inactivation.

[b] ND, not detected.

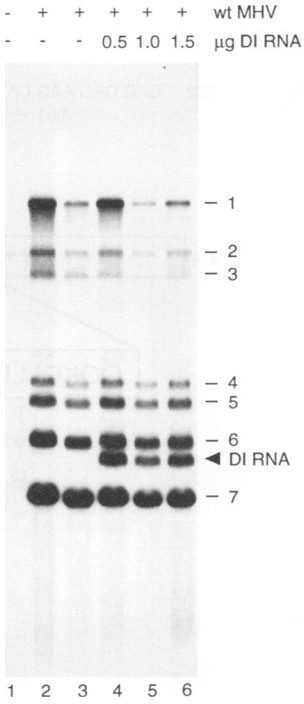

FIG. 3. Replicative ability of synthetic DI RNA. L2 cells were infected with wild-type (wt) virus and then were transfected with the indicated amount of DI RNA (lanes 4 to 6) or with H_2O in two independent controls (lanes 2 and 3). Mock-infected, mock-transfected L2 cells provided an additional control (lane 1). Transfected L2 cells were then plated onto a monolayer of 17Cl1 cells, and viral RNA was labeled from 13 to 15 h postinfection with 333 μCi of $^{32}P_i$ per ml in phosphate-free medium in the presence of 20 μg of actinomycin D per ml. Total cytoplasmic RNA was purified, electrophoresed on 1% agarose, and visualized by autoradiography. MHV genomic RNA1, subgenomic RNA2 to RNA7, and DI RNA are indicated.

purified plaque of Alb25 (data not shown). Thus, we tentatively conclude that the lesion in Alb25 does not map in the N gene or that it maps too close to the 5′ end of the N gene for an appreciable rate of recombination to occur with the donor RNA used. Another mutant, Alb11, which was of intermediate thermolability, also did not appear to be an N mutant (data not shown).

Replicative ability of synthetic DI RNA. The construction of pB36 was based on the assumption that RNA synthesized from this vector would function as replicating DI RNA, as does the authentic BCV DI RNA after which it was patterned (6). The high efficiency of pB36-derived RNA as a donor for RNA recombination was consistent with this assumption. To test this notion more directly, we infected cells with wild-type MHV and transfected them with putative DI RNA under conditions similar to those used in the mapping experiments. Infected/transfected cells were then radiolabeled with $^{32}P_i$ in the presence of actinomycin D to detect synthesis of viral RNA species, which were resolved by agarose gel electrophoresis. As shown in Fig. 3, infected cells that were transfected with pB36 RNA abundantly synthesized an extra RNA species of the size expected for the synthetic DI RNA, in addition to the seven MHV RNAs. The nonpolyadenylated sizes of MHV-A59 RNA6 and RNA7 are 1,745 and 2,446 nt, respectively; the predicted nonpolyadenylated size of pB36 RNA is 2,183 nt. This clearly established that the putative synthetic DI RNA is, indeed, a replicative entity in the presence of helper virus.

Sequence of the Alb1 N gene. The entire Alb1 N gene sequence, as well as the sequences of flanking regions consisting of 290 nt of the M gene and 225 nt of the 3′ UTR, were determined from cDNA clones. Two nucleotide differences were found with respect to the MHV-A59 wild-type N gene sequence (27; GenBank accession number, M35256): nt 368 was changed from T to G, and nt 378 was changed from G to T (Fig. 4A). This resulted in two closely linked amino acid changes: leucine 123 was changed to arginine, and tryptophan 126 was changed to cysteine (Fig. 4B). These mutations fall in the latter portion of the first domain of a proposed three-domain model for the MHV N protein (23, 27) and are well separated from the deleted region responsible for the phenotype of the previously characterized N mutant, Alb4. No other changes were found in the sequenced portions of Alb1, except that the final codon of the M gene was ACC instead of the previously determined AUC (2), resulting in a threonine instead of an isoleucine at this position. However, the ACC codon also occurs in our wild-type MHV-A59 virus (29), as well as in all other derived mutants and revertants that we have examined, and thus this probably represents a difference between laboratory strains of MHV-A59.

Analysis of revertants of Alb1. To determine whether one or both of the mutations in the Alb1 N gene is responsible for the phenotype of this mutant, we isolated and analyzed revertants. Because Alb1 is weakly viable at the nonpermissive temperature, it was not possible to detect revertants by direct titer determination in virus stocks at 39°C (Table 2). Revertants were instead obtained by twice passaging independent stocks of Alb1 at the nonpermissive temperature and then selecting, via a thermal inactivation step, survivors that formed large (wild-type-sized) plaques at the nonpermissive temperature. This procedure did not allow us to rigorously establish a reversion frequency for Alb1, but from Table 2 and similar experiments, we can estimate that it is less than 5×10^{-5}.

For the first revertant obtained, Alb1RevA, the entire N gene and flanking sequences were determined from cDNA

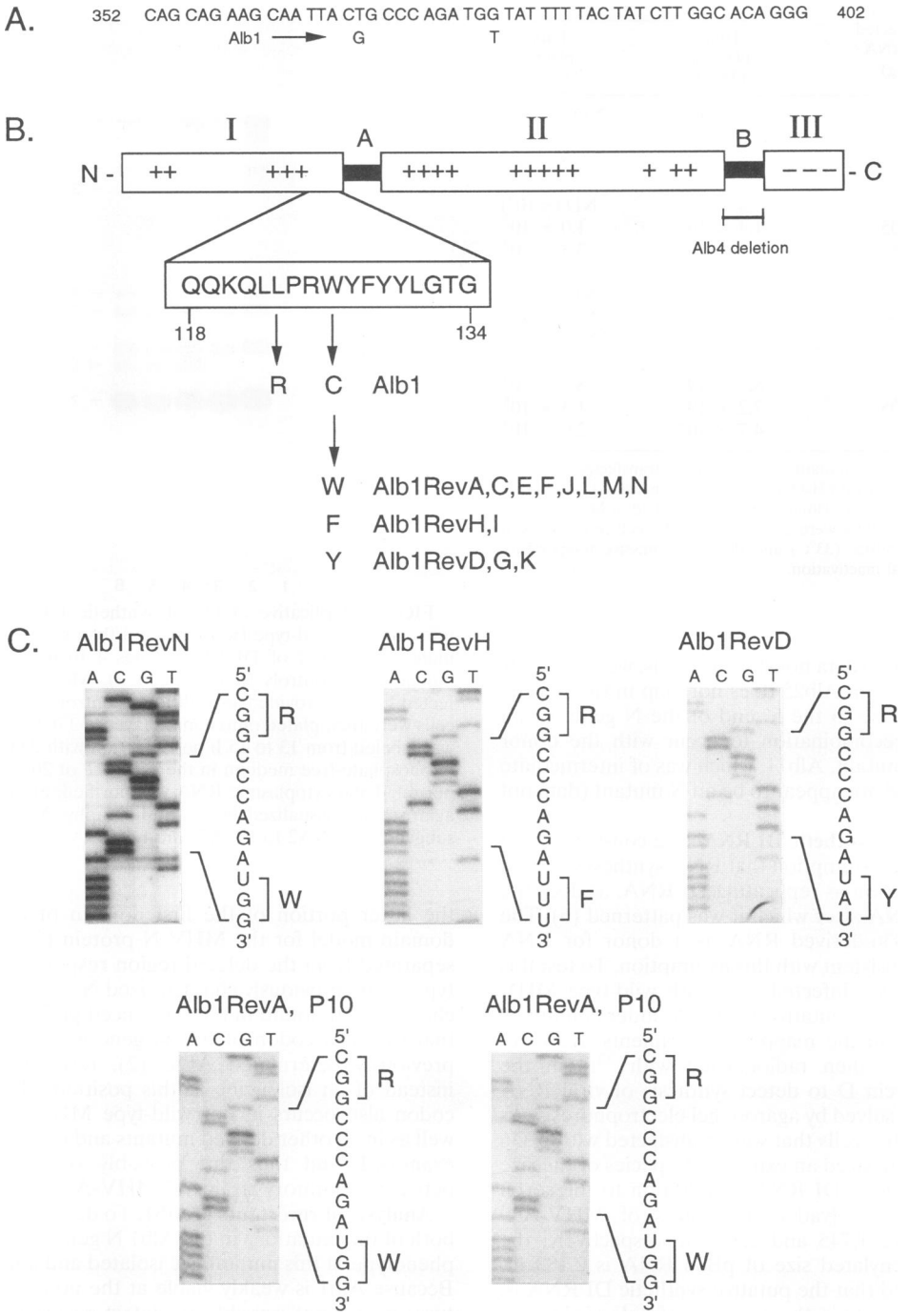

FIG. 4. N gene and protein sequence of the Alb1 mutant and revertants. (A) A portion of the coding region of the wild-type MHV-A59 N gene; numbering begins with the first base of the start codon. The two nucleotide changes in the Alb1 N gene are indicated beneath the wild-type sequence. (B) A region of the MHV-A59 N protein sequence, showing the two amino acid residues changed in the Alb1 N protein and the three types of residue changes in each of 13 revertants. The sequence is given in the context of a previously proposed three-domain model of the MHV N protein (27). Also shown is the locus of the deletion in the mutant Alb4 (16). (C) The relevant portion of the sequence of RNA from cells infected with a representative of each of the three classes of revertants (Alb1RevN, Alb1RevH, and Alb1RevD) and from cells infected with two independent stocks of Alb1RevA that had been serially passaged 10 times at the nonpermissive temperature, 39°C. The indicated segment of sequence for each is given as positive-sense RNA.

clones as they had been for Alb1. A single-base change relative to Alb1 was found, changing codon 126 back to the wild-type UGG, encoding tryptophan. This result, taken together with the mapping result, established that the W126C mutation alone was responsible for the phenotype of Alb1 and that the L123R mutation was phenotypically silent. For 12 additional revertants, Alb1RevC to Alb1RevN, direct RNA sequencing of the region of the Alb1 mutations reinforced this conclusion (Fig. 4B and C). Revertants fell into three classes, all of them changing codon 126 to the wild-type UGG (tryptophan) or to the conservatively substituted UUU (phenylalanine) or UAU (tyrosine). One revertant, designated Alb1RevB, was anomalous in that both codons 123 and 126 were changed back to their wild-type counterparts. This raised the possibility that viruses harboring the L123R mutation were at a selective disadvantage with respect to the wild type and that Alb1RevB might be the only representative of a class of "complete" revertants of Alb1. To test this, we serially passaged two independent stocks of Alb1RevA 10 times at the nonpermissive temperature to see whether a detectable fraction of the resulting selected virus population by passage 10 would contain a codon other than CGG (arginine) at position 123. As shown in Fig. 4C, however, this clearly did not occur. Thus, although it is possible that Alb1RevB arose under unique selective conditions, the most consistent explanation is that it was a wild-type contaminant. This question will be resolvable only if an additional silent marker mutation is found elsewhere in the genome of Alb1.

DISCUSSION

The results presented in this paper have immediate practical implications for the construction of site-specific mutations in the genome of MHV. We previously demonstrated that targeted RNA recombination between the mutant Alb4 and cotransfected synthetic RNA7 allowed the selection of progeny recombinant viruses at a frequency on the order of 10^{-5} (16). In the present work we show that, by using a synthetic DI RNA as the donor RNA species, the efficiency of recovery of recombinants was increased by at least 2 orders of magnitude. Our observed frequencies of recombinants (Table 1), both under conditions of heat selection (up to 80% of selected survivors) and in the absence of selection (up to 10% of total viral progeny), accord well with those of Van der Most et al. (42), who have demonstrated targeted recombination when using donor RNA from a variant of a cloned natural MHV DI. These workers observed a 95% efficiency of incorporation of a genetic marker into Alb4 following selection of recombinants at the nonpermissive temperature and an efficiency on the order of 1% for the incorporation of unselected markers into the 5′ end of the genome of wild-type MHV. On the basis of genetic crosses among a large number of temperature-sensitive mutants, Baric et al. (4) estimated a recombination frequency of 1% per 1,300 nt of the MHV genome. It is noteworthy that our targeted recombination frequencies are in substantial agreement with this value, to the extent that the two different types of experiments can be compared.

The increased rate of recombination obtained with synthetic DI RNA as the donor RNA was sufficiently high to allow us to directly identify recombinants without the necessity of selection by thermal inactivation. For the future construction of mutant viruses, this offers the advantage of a simplified protocol for targeted recombination. More importantly, it may also allow the identification of recombinant mutants that are still partially temperature sensitive or thermolabile, thus expanding the applicability of this technique. As well, the optimized recombination frequency may be high enough to allow selection of recombinants generated by more than one crossover between genomic and synthetic input RNA. Such multiple crossovers, which are common in mixed infections with two different strains of MHV (19), would allow the engineering of mutations into sites in the MHV genome distant from the 5′ or 3′ terminus.

RNA synthesized from the transcription vector pB36 gave rise to much larger numbers of recombinants than RNA7 and also appeared to inhibit the replication of MHV. These two properties strongly suggested that pB36-derived RNA truly acted as an efficiently replicating DI RNA. Direct labeling of viral RNA synthesis in MHV-infected cells transfected with pB36 RNA demonstrated this supposition to be correct. The putative synthetic DI RNA was replicated to a level comparable to that of RNA6, one of the more abundant MHV subgenomic RNA species (Fig. 3). This indicates that as little as 467 nt from the 5′ end of the MHV genome is sufficient to support DI RNA replication. It should be noted that this encodes only slightly more than one-third of p28, the proteolytically processed amino-terminal product of MHV gene 1 (8, 38). Thus, it is unlikely that the MHV 5′-end sequence requirement for DI RNA replication reflects a requirement for a function provided by p28. Rather, it is more probable that at least part of the promoter for positive-strand RNA synthesis resides in some portion of the genomic sequence beyond the leader region. Alternatively, or in addition, some extent of the beginning of the gene 1 open reading frame may be necessary owing to the currently poorly understood apparent coupling between DI replication and translation (7, 15).

Recombinants obtained between Alb4 and either synthetic RNA7 or synthetic DI RNA most probably arise from single-crossover events that result when a replicating RNA polymerase switches templates during synthesis of full-length genome or its minus-strand complement. This could happen either (i) via a crossover from synthetic RNA template to genome RNA template during negative-strand RNA synthesis or (ii) via a crossover from genome-length minus-strand RNA template to the minus-strand complement of synthetic RNA during positive-strand RNA synthesis. Since neither of these mechanisms directly requires that the synthetic RNA contain a functional promoter for positive-strand RNA synthesis, the recombinational advantage of DI RNA compared with RNA7 is most probably simply due to a larger population of the DI RNA brought about by its ability to replicate. Alternatively, more complex considerations may dictate relative recombinational ability. It is conceivable that some element present in DI RNA but not in RNA7 may be critical for sequestration and alignment of RNA templates in replicating polymerase complexes with genomic RNA.

Mechanistic considerations aside, we expect pB36 and vectors derived therefrom to provide useful tools both in the construction of new MHV mutants and in the mapping of the mutations in MHV mutants previously obtained by classical approaches. One example of the latter has been demonstrated in this report. The lesion in the temperature-sensitive and thermolabile mutant Alb1 was shown to map to the N gene. The Alb1 N sequence contains two closely linked point mutations, and these fall in the most highly conserved portion among the coronavirus N proteins (Fig. 5). This region was first noted as being the most homologous stretch of amino acid sequence between the N proteins of avian infectious bronchitis virus and MHV (5); this observation has held true for all subsequently determined coronavirus N protein sequences, suggesting an important functional role. Of the two mutations in the Alb1 N protein, one (W126C) occurs at a position that

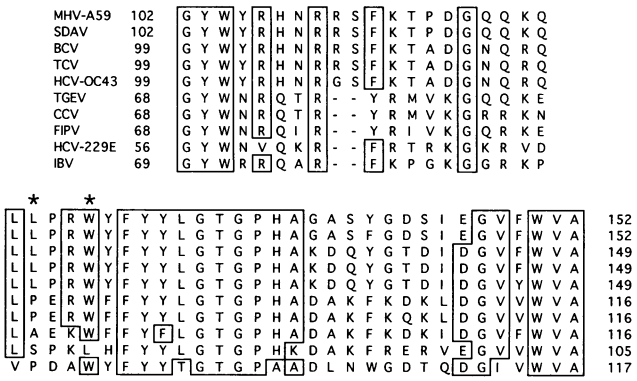

FIG. 5. Region of highest homology among all coronavirus N proteins. Boxed residues are those that are identical in 7 or more of the 10 N protein sequences for MHV-A59 (27), the rat coronavirus sialodacryoadenitis virus (SDAV) (17), BCV (20), turkey enteric coronavirus (TCV) (44), human coronaviruses (HCV) strains OC43 (13) and 229E (35), porcine transmissible gastroenteritis virus (TGEV) (14), canine coronavirus (CCV) (11), feline infectious peritonitis virus (FIPV) (43), and avian infectious bronchitis virus (IBV) (5). The two residues mutated in Alb1 are indicated by asterisks.

is more highly conserved than the other (L123R) (Fig. 5). The analysis of 13 independent revertants of Alb1 indicates that W126C is the critical mutation in Alb1 and that the L123R mutation is phenotypically silent. The W126C mutation falls in a block of five aromatic residues, WYFYY, that may be essential in forming a hydrophobic interface between N monomers, between N and M proteins, or between N and a cellular membrane (1). Each of the revertants of Alb1 exactly restores the first residue of this block or conservatively replaces it. It must be noted, however, that the mutation that gives rise to the W126C change also alters a residue in the internal (I) open reading frame contained in the +1 reading frame within the N gene (27). It has been shown for BCV that the I protein is expressed in infected cells, but it is not yet clear whether I is a viral structural protein (36). Thus, at this time it cannot be ruled out that the relevant lesion in Alb1 is in the I protein, not the N protein. These possibilities remain to be sorted out by biochemical and genetic means. It is hoped that such further characterization of Alb1 will provide useful insights into MHV N protein structure and function.

ACKNOWLEDGMENTS

We are grateful to Ruey-Yi Chang and David Brian for communication of unpublished results, and we are indebted to Stanley Sawicki for helpful advice on labeling viral RNA. We thank Lawrence Sturman for providing the Alb mutants and for many valuable discussions. We thank Tim Moran, Molecular Genetics Core Facility, Wadsworth Center, for the synthesis of oligonucleotides.

This work was supported in part by Public Health Service grant AI31622 from the National Institutes of Health.

REFERENCES

1. **Anderson, R., and F. Wong.** 1993. Membrane and phospholipid binding by murine coronaviral nucleocapsid N protein. Virology **194:**224–232.
2. **Armstrong, J., H. Niemann, S. Smeekens, P. Rottier, and G. Warren.** 1984. Sequence and topology of a model intracellular membrane protein, E1 glycoprotein, from a coronavirus. Nature (London) **308:**751–752.
3. **Banerjee, A. K., D. P. Rhodes, and D. S. Gill.** 1984. Complete nucleotide sequence of the mRNA coding for the N protein of vesicular stomatitis virus (New Jersey serotype). Virology **137:**432–438.
4. **Baric, R. S., K. Fu, M. C. Schaad, and S. A. Stohlman.** 1990. Establishing a genetic recombination map for murine coronavirus strain A59 complementation groups. Virology **177:**646–656.
5. **Boursnell, M. E. G., M. M. Binns, I. J. Foulds, and T. D. K. Brown.** 1985. Sequences of the nucleocapsid genes from two strains of avian infectious bronchitis virus. J. Gen. Virol. **66:**573–580.
6. **Chang, R.-Y., and D. Brian.** 1993. Unpublished data.
7. **De Groot, R. J., R. G. Van der Most, and W. J. M. Spaan.** 1992. The fitness of defective interfering murine coronavirus DI-a and its derivatives is decreased by nonsense and frameshift mutations. J. Virol. **66:**5898–5905.
8. **Denison, M. R., and S. Perlman.** 1986. Translation and processing of mouse hepatitis virus virion RNA in a cell-free system. J. Virol. **60:**12–18.
9. **Fichot, O., and M. Girard.** 1990. An improved method for sequencing of RNA templates. Nucleic Acids Res. **18:**6162.
10. **Gubler, U., and B. J. Hoffman.** 1983. A simple and very efficient method for generating cDNA libraries. Gene **25:**263–269.
11. **Horsburgh, B. C., I. Brierly, and T. D. K. Brown.** 1992. Analysis of a 9.6 kb sequence from the 3′ end of canine coronavirus genomic RNA. J. Gen. Virol. **73:**2849–2862.
12. **Jeong, Y. S., and S. Makino.** 1992. Mechanism of coronavirus transcription: duration of primary transcription initiation activity and effects of subgenomic RNA transcription on RNA replication. J. Virol. **66:**3339–3346.
13. **Kamahora, T., L. H. Soe, and M. M. C. Lai.** 1989. Sequence analysis of nucleocapsid gene and leader RNA of human coronavirus OC43. Virus Res. **12:**1–9.
14. **Kapke, P. A., and D. A. Brian.** 1986. Sequence analysis of the porcine transmissible gastroenteritis coronavirus nucleocapsid protein gene. Virology **151:**41–49.
15. **Kim, Y.-N., M. M. C. Lai, and S. Makino.** Generation and selection of coronavirus defective interfering RNA with large open reading frame by RNA recombination and possible editing. Virology **194:**244–253.
16. **Koetzner, C. A., M. M. Parker, C. S. Ricard, L. S. Sturman, and P. S. Masters.** 1992. Repair and mutagenesis of the genome of a deletion mutant of the coronavirus mouse hepatitis virus by targeted RNA recombination. J. Virol. **66:**1841–1848.
17. **Kunita, S., M. Mori, and E. Terada.** 1993. Sequence analysis of the nucleocapsid protein gene of rat coronavirus SDAV-681. Virology **193:**520–523.
18. **Lai, M. M. C.** 1990. Coronavirus: organization, replication, and expression of genome. Annu. Rev. Microbiol. **44:**303–333.
19. **Lai, M. M. C.** 1992. RNA recombination in animal and plant viruses. Microbiol. Rev. **56:**61–79.
20. **Lapps, W., B. G. Hogue, and D. A. Brian.** 1987. Sequence analysis of the bovine coronavirus nucleocapsid and matrix protein genes. Virology **157:**47–57.
21. **Liljeström, P., S. Lusa, D. Huylebroeck, and H. Garoff.** 1991. In vitro mutagenesis of a full-length cDNA clone of Semliki Forest virus: the small 6,000-molecular-weight membrane protein modulates virus release. J. Virol. **65:**4107–4113.
22. **Makino, S., F. Taguchi, N. Hirano, and K. Fujiwara.** 1984. Analysis of genomic and intracellular viral RNAs of small plaque mutants of mouse hepatitis virus JHM strain. Virology **139:**138–151.
23. **Masters, P. S.** 1992. Localization of an RNA-binding domain in the nucleocapsid protein of the coronavirus mouse hepatitis virus. Arch. Virol. **125:**141–160.
24. **Masters, P. S., C. A. Koetzner, D. Peng, M. M. Parker, C. S. Ricard, and L. S. Sturman.** Site-directed mutagenesis of the genome of mouse hepatitis virus by targeted RNA recombination. Adv. Exp. Med. Biol., in press.
25. **Melton, D. A., P. A. Krieg, M. R. Rebagliati, T. Maniatis, K. Zinn, and M. R. Green.** 1984. Efficient in vitro synthesis of biologically active RNA and RNA hybridization probes from plasmids containing a bacteriophage SP6 promoter. Nucleic Acids Res. **12:**7035–7056.
26. **Pachuk, C. J., P. J. Bredenbeek, P. W. Zoltick, W. J. M. Spaan, and S. R. Weiss.** 1989. Molecular cloning of the gene encoding the

putative polymerase of mouse hepatitis coronavirus, strain A59. Virology **171:**141–148.
27. **Parker, M. M., and P. S. Masters.** 1990. Sequence comparison of the N genes of five strains of the coronavirus mouse hepatitis virus suggests a three domain structure for the nucleocapsid protein. Virology **179:**463–468.
28. **Racaniello, V. R., and D. Baltimore.** 1981. Cloned poliovirus cDNA is infectious in mammalian cells. Science **214:**916–919.
29. **Ricard, C. S., C. A. Koetzner, P. S. Masters, and L. S. Sturman.** Unpublished data.
30. **Rice, C. M., R. Levis, J. H. Strauss, and H. V. Huang.** 1987. Production of infectious RNA transcripts from Sindbis virus cDNA clones: mapping of lethal mutations, rescue of a temperature-sensitive marker, and in vitro mutagenesis to generate defined mutations. J. Virol. **61:**3809–3819.
31. **Sambrook, J., E. F. Fritsch, and T. Maniatis.** 1989. Molecular cloning: a laboratory manual, 2nd ed. Cold Spring Harbor Laboratory Press, Cold Spring Harbor, N.Y.
32. **Sanger, F., S. Nicklen, and A. R. Coulson.** 1977. DNA sequencing with chain-terminating inhibitors. Proc. Natl. Acad. Sci. USA **74:**5463–5467.
33. **Sawicki, S. G., and D. L. Sawicki.** 1986. Coronavirus minus-strand RNA synthesis and effect of cycloheximide on coronavirus RNA synthesis. J. Virol. **57:**328–334.
34. **Sawicki, S. G., and D. L. Sawicki.** 1990. Coronavirus transcription: subgenomic mouse hepatitis virus replicative intermediates function in RNA synthesis. J. Virol. **64:**1050–1056.
35. **Schreiber, S. S., T. Kamahora, and M. M. C. Lai.** 1989. Sequence analysis of the nucleocapsid protein gene of human coronavirus 229E. Virology **169:**142–151.
36. **Senanayake, S. D., M. A. Hofmann, J. L. Maki, and D. A. Brian.** 1992. The nucleocapsid protein gene of bovine coronavirus is bicistronic. J. Virol. **66:**5277–5283.
37. **Sethna, P. B., S.-L. Hung, and D. A. Brian.** 1989. Coronavirus subgenomic minus-strand RNAs and the potential for mRNA replicons. Proc. Natl. Acad. Sci. USA **86:**5626–5630.
38. **Soe, L. H., C.-K. Shieh, S. C. Baker, M.-F. Chang, and M. M. C. Lai.** 1987. Sequence and translation of the murine coronavirus 5′-end genomic RNA reveals the N-terminal structure of the putative RNA polymerase. J. Virol. **61:**3968–3976.
39. **Spaan, W., D. Cavanagh, and M. C. Horzinek.** 1988. Coronaviruses: structure and genome expression. J. Gen. Virol. **69:**2939–2952.
40. **Sturman, L. S., C. Eastwood, M. F. Frana, C. Duchala, F. Baker, C. S. Ricard, S. G. Sawicki, and K. V. Holmes.** 1987. Temperature-sensitive mutants of MHV-A59. Adv. Exp. Med. Biol. **218:**159–168.
41. **Sturman, L. S., and K. V. Holmes.** 1983. The molecular biology of coronaviruses. Adv. Virus Res. **28:**35–111.
42. **Van der Most, R. G., L. Heijnen, W. J. M. Spaan, and R. J. de Groot.** 1992. Homologous RNA recombination allows efficient introduction of site-specific mutations into the genome of coronavirus MHV-A59 via synthetic co-replicating RNAs. Nucleic Acids Res. **20:**3375–3381.
43. **Vennema, H., R. J. de Groot, D. A. Harbour, M. C. Horzinek, and W. J. M. Spaan.** 1991. Primary structure of the membrane and nucleocapsid protein genes of feline infectious peritonitis virus and immunogenicity of recombinant vaccinia viruses in kittens. Virology **181:**327–335.
44. **Verbeek, A., and P. Tijssen.** 1991. Sequence analysis of the turkey enteric coronavirus nucleocapsid and membrane protein genes: a close genomic relationship with bovine coronavirus. J. Gen. Virol. **72:**1659–1666.